Stability metrics and improved odometry prediction for tracked vehicles with tactile sensors

Raimund Edlinger[1], Christoph Föls[1], Roman Froschauer[1] and Andreas Nüchter[2]

***Abstract*— In this paper, we address the motion efficiency in autonomous robot exploration with tracked vehicles in rough terrain. Tracked vehicles, along with wheel-driven propulsion systems, are the preferred platform for Unmanned Ground Vehicles (UGVs) in poor terrain conditions. However, these robots have problems with cornering, turning maneuvers or rotation around the central axis. Depending on the coefficient of friction between the tracks and the ground, the total weight and center of mass tracked vehicles produce higher slip, purely accurate and reliable pose estimation. To improve the direction of motion and the prediction of the resulting track forces and odometry calculation for tracked vehicles, a tactile surface sensor was developed to provide improved odometry determination for different ground conditions. The integration of the measurement data of the pressure sensor and the use of an improved model to determine the contact points and to improve the odometry calculation are the main objectives of this work. This is achieved by calculating the centre of gravity of the two tracks separately, using the measurement data of the pressure sensor and the local coordinates (x,y) of each of the measurement points. The sensor concept was tested and evaluated on different grounds and terrains. The system can be used as a predictive model for tracked vehicle traversability and to ensure a stable position when straight manipulation tasks must be performed on rough terrain.**

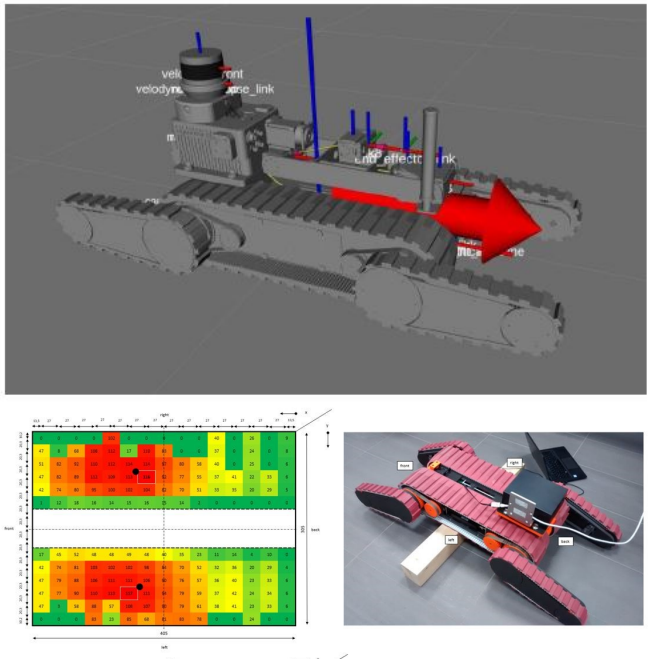

Fig. 1. URDF model and stability vector (top); pressure distribution on bars (bottom)

I. INTRODUCTION

The automation of robots and vehicles is becoming increasingly important in many different industries. Companies are trying to retrofit existing vehicles and develop autonomous assistance functions or complete autonomy skills. Most vehicles and robotic systems are equipped with different sensor modalities to achieve the best possible sensor coverage and redundancy. However, most robotic systems lack the feedback of steadiness and stability. Legged robots are the exception, as pressure sensors are usually installed at the feet. The advanced and new generation of humanoid and legged robots has not only the versatility, but also the reliability and robustness. These features are achieved through some kind of force or torque control - either through integrated load cells in the joints or through pressure sensors on the end-effectors to properly control the interaction forces with the environment [1], [2]. Many applications which are to be automated can be addressed with ordinary sensors. For example, an inertial measurement sensor can be used to determine the position and orientation of the robot. When moving in rough terrain or climbing steep stairs $> 45°$, a feedback of the stability of the robot can be essential. Tracked vehicles, along with wheel-driven propulsion systems, are the preferred platform for UGVs in poor terrain conditions or harsh environments. However, a tracked vehicle concept also has disadvantages, especially during cornering maneuvers or turning maneuvers around the instantaneous center of rotation (ICR). Depending on the coefficient of friction between the tracks and the ground and the total weight and center of gravity of the vehicle, such models produce high slip and shift of the trajectory. A precise prediction of the resulting track on the basis of the current terrain situation would increase the control/steering stability of autonomous or even remote operated vehicles. Therefore this paper presents a tactile surface sensor to provide improved odometry determination for different ground conditions. The key question to be answered is how to determine the resulting position after actuating the right and left tracks independently to perform turns etc. or in other words: If a robot starts from a position p, and the right and left tracks move respective distances Δs_r and Δs_l, the question is always: What is the resulting new position p'? Odometry is obtained by integrating wheel encoders for each

[1]Raimund Edlinger, Christoph Föls and Roman Froschauer are with Faculty of Electrical Engineering, Mathematics and Computer Science, University of Applied Sciences Upper Austria, 4600 Wels, Austria raimund.edlinger@fh-wels.at

[2]Andreas Nüchter is with Faculty of Informatics VII Robotics and Telematics, Julius-Maximilians University Würzburg andreas.nuechter@uni-wuerzburg.de

track which occurs following odometry error sources:

- Limited encoder resolution (deterministic)
- Belt coating (deterministic)
- Unequal track diameter (deterministic)
- Variation in the contact point of tracks (deterministic)
- Unequal floor contact and variable friction can lead to slipping (non deterministic)

Deterministic errors can be eliminated by appropriate calibration, whereas non-deterministic errors must be described by error models and will always lead to an uncertain pose estimation.

II. RELATED WORK

Localization is one of the important attributes, along with mapping and perception methods, when automating vehicles. Besides LIDAR and visual odometry, GNSS systems are considered as basic equipment for mobile UGVs. In addition, each mobile robot provides internal odometry data depending on the kinematic. Due to the simplicity the odometry is often used to calculate the pose estimation for wheeled and tracked vehicles. The calculation integrates the rotational speed of the wheel or track, which makes the accuracy of the calculated position dependent on the sampling rate and on the slip between the ground and the contact area. When moving UGVs, the accuracy of localization depends not only on the supporting points but also on the center of gravity of the robot. Especially on loose ground (sand, gravel) or on flat terrain (wood, tiles), the localization accuracy of odometry decreases significantly due to slip. Several studies already improved models vehicle model identification [3], [4], [5] and for slip estimation and compensation [6], [7], [8] and utilize kinematic models. Approaches for online slip model identification have been implemented in [9]. Many researchers use IMU in combination with sensor-based technologies [10], such as GNSS, encoders, or cameras with an EKF Filter for sensor fusion [11].
In contrast to previous approaches, this work has attempted to develop a sensor that improves the odometry calculation and telemetry data using a new tactile sensor design.

III. SENSOR CONCEPT

The system can be further used as a predictive model for tracked vehicle traversability and to ensure a stable position when straight manipulation tasks must be performed on rough terrain.

A. Tactile Sensor Design

A tactile sensor is modeled on the human sense of touch and measures physical states and properties through contact between the sensor and the object. Contact is not only understood as physical contact, but also includes the shape, temperature, structure, hardness, moisture content, etc. of the object. Tactile sensors are mainly mounted on gripper arms of robots and can be used to determine the gripping force or the distribution of the force. This is important because this force control allows an object to be held securely and prevents it from being damaged. The construction of the flexible pressure sensor was realized using the so-called sandwich construction method, i.e. the foil is sandwiched between two conductive materials. In order to be able to test individual pressure points better or more clearly this paper presents the characteristic of a 15 × 15 sensor matrix based on velostat for ground pressure distribution measurements. The velostat is a pressure-sensitive conductive foil, so that the resistance can change when pressure is applied and thus flexible sensors can be produced. The velostat polymer foil is placed between the copper foils, which are again arranged 90 degrees to each other, see schematic illustration in **??**. The columns and rows form crossing points, which can be called measuring points. The resistance R_{velo} is measured there with the aid of a voltage divider.

$$R_{velo} = R_H \left(\frac{U_{Measure}}{U_{Total}} - 1 \right)$$

Fig. 2 shows the schematic structure of the 5-layer pressure sensor unit:

- L1: Anti slip mat
- L2: Copper foil arrangement 90 degrees to the direction of travel
- L3: Pressure sensitive conductive foil velostat
- L4: Copper foil arrangement in direction of travel
- L5: Anti slip mat

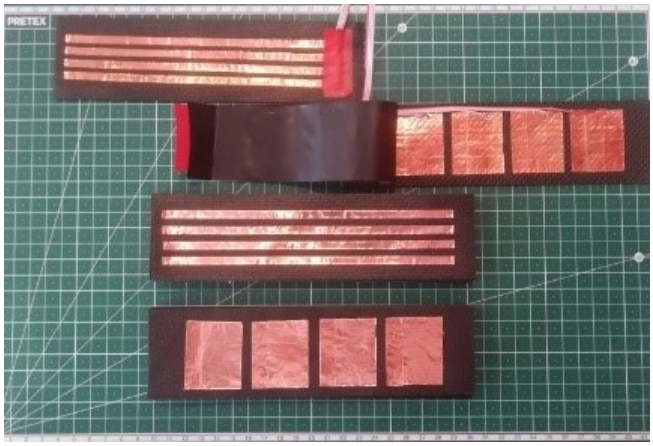

Fig. 2. Interactive pressure sensor structure

Flexible sensors have been studied in detail several times due to their great potential for wearable electronic applications [12]. This potential has now been applied to complex robotic systems for detection and ground contact analysis. Fig. 3 shows the basic structure of the developed sensor system. The sensor data are sampled in a cycle of 200ms and calibrated to the value zero after initialisation. The sensor values are then filtered and converted to an 8-bit variable, with 0 (no contact) and 255 (maximum contact) defined.

The respective copper columns and copper rows are read in with two 16 channel analog multiplexer and processed on an ESP32 from espressif[1].

[1]https://www.espressif.com/en/products/socs/esp32

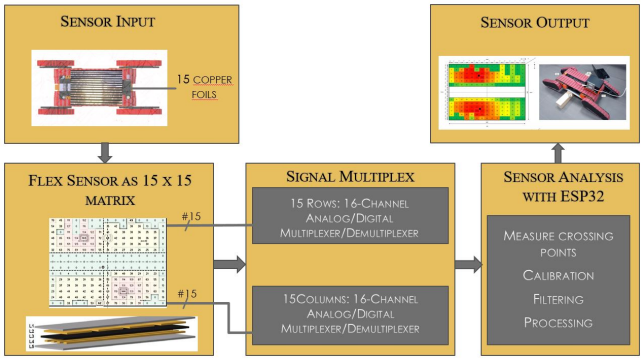

Fig. 3. Overview of signal processing and flexible pressure sensor structure

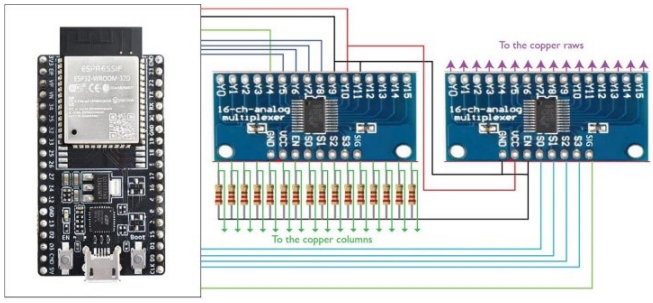

Fig. 4. Electrical circuit

The 16-channel analog-digital multiplexer boards can be used when there are many analog inputs in a circuit, as in the case with the force sensor for the centre drives (15x15 matrix). In this case, one of these inputs must be selected and processed each time. This multiplexer can be used to select 16 analogue inputs. There are four S0-3 pins that set one of the analog inputs as an output on the SIG pin by entering corresponding values, see fig. 4.

IV. METHOD

A. Robot model and MARC Payload

The developed rescue robot offers the possibility of individual configuration of sensor and actuator modules. These modules are automatically recognised and the current configuration is specified in the XML-based robot description file. This modular design has the advantage that the robot can be optimally configured and equipped for the respective application in a very short time [13]. The robot base and the already developed modules are each stored with a configuration file in which the mass, dimensions, centre of gravity matrix and collision model are specified.

B. Stability metrics

Based on the robot and payload configuration file this concept incorporates a model to measure the current vehicle roll dynamics, the current center of mass (CoM) from the entire robot system, the stability index (SI), inertia measurement unit data and the vehicle rollover propensity (M_K). The CoM calculation reads the robot description from the ROS Unified Robot Description Format (URDF) parameter server and calculate the total mass of robot system. In the loop it calculates part of CoM equation depending on links and transform the point at which the distribution of mass is equal in all directions which does not depend on gravitational field. The resulting Zero-Moment Point (ZMP) prediction provides a direct measure of the vehicle stability index (SI).

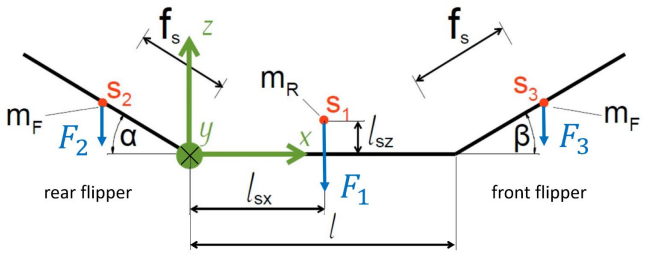

Fig. 5. Skeleton of the robot

TABLE I
VEHICLE GEOMETRY PARAMETERS

α	current flipper angle front
β	current flipper angle front
s_i	center of mass $s_{i=1...3}$ chassis and flippers
F_i	weight forces $F_{i=1...3}$ chassis and flippers
f_s	CoM distance flipper from pivot point
l	length of robot chassis in x-direction
l_{sx}	CoM distance chassis from coordinate system in x-direction
l_{sz}	CoM distance chassis from coordinate system in z-direction
m_F	mass of flipper
m_R	mass of chassis
m_T	total mass of robot
A_s	ground contact area per side (s)
l_s	track length
b	vehicle width
p	pressure as uniform normal pressure distribution
c	apparent cohesion
ϕ	angle of internal shearing resistance of terrain
k_c, k_ϕ	pressure sinkage parameter
n	exponent of deformation
ω_s	pressure sinkage parameter
z	sinkage
n_p	number of periods

IMU-Data: A built-in IMU (Inertial Measurement Unit) can provide sufficient information about the body's specific force, angular rate and orientation based on acceleration, gyroscope and magnetometer data.
CoM: The center of mass of the robot base including both flippers without manipulator and sensor module can be calculated by

$$\overrightarrow{CoM} = \begin{pmatrix} x_s \\ y_s \\ z_s \end{pmatrix} = \frac{1}{\sum_{i=1}^{\infty} m_i} \left(\begin{pmatrix} x_1 \\ y_1 \\ z_1 \end{pmatrix} m_1 + \begin{pmatrix} x_2 \\ y_2 \\ z_2 \end{pmatrix} m_2 + \cdots \right)$$

$$= \frac{1}{m_R + 2 \cdot m_F} \begin{pmatrix} m_R \cdot l_{sx} + m_F \cdot (l + f_s \cdot (\cos\beta - \cos\alpha)) \\ (m_R + 2 \cdot m_F) \cdot l_{sy} \\ m_R \cdot l_{sz} + m_F \cdot f_s \cdot (\sin\alpha + \sin\beta) \end{pmatrix} \quad (1)$$

The tilting moment M_K and the stability torque M_S for the rear are

$$\underbrace{F_2 \cdot f_s \cos\alpha}_{M_K} < \underbrace{F_1 \cdot l_{sx} + F_3 \cdot (l + f_s \cos\beta)}_{M_S} \tag{2}$$

respectively for the front

$$\underbrace{F_3 \cdot f_s \cos\beta}_{M_K} < \underbrace{F_1 \cdot (l - l_{sx}) + F_2 \cdot (l + f_s \cos\alpha)}_{M_S} \tag{3}$$

SI: Hence, the stability index (SI) is given by

$$SI = \frac{M_S}{M_K} > 1 \tag{4}$$

C. Previous approaches for kinematic and probabilistic terrain and motion modelling

For field robot applications the terrain characterization is essential to model the pressure-sinkage relationship for homogeneous terrain proposed by Bekker [14]

$$p = \left(\frac{k_c^{'}}{b} + k_\phi\right) z^n$$

or with a newer equation from Reece [15]

$$p = (ck_c^{'} + \gamma_s b k_\phi^{'}) \left(\frac{z}{b}\right)^n$$

Depending on the designed tracks a sinusoidal pressure distribution can be modeled as [16]

$$p = \frac{m_T}{b l_s}\left(1 + \cos\frac{2n_p \pi x}{l}\right)$$

A general approach for the sinking as resistance to motion is given by

$$z_0 = \left(\frac{p}{\frac{k_c}{b} + k_\phi}\right)^{1/n} = \left(\frac{\frac{m_T}{b l_s}}{\frac{k_c}{b} + k_\phi}\right)^{1/n}$$

A uniform pressure distribution can be calculated for the terrain compaction R_c with

$$R_c = \frac{1}{(n+1) b^{1/n} \left(\frac{k_c}{b} + k_\phi\right)^{1/n}} \left(\frac{m_T}{l}\right)^{(n+1)/n}$$

In this paper, we propose an kinematic model for ICR and extended odometry prediction based on the detection of support points for tracked vehicles. To improve the accuracy for tracked vehicles in such environments, the paper focuses on estimating the interaction between a vehicle and the ground. Modeling odometry estimation depends on many terrain-specific parameters in addition to robot parameters, see table I. Based on [16] a skid-steering model for a simplified analysis of the turning behaviour of a tracked vehicles is used. The maximum tractive effort T_{max} for vehicles with tracks is defined with the parameters in table I

$$F_{max} = A_s c + m_T \tan\phi$$

The following equation indicates a uniform normal pressure distribution and the total tractive effort of a track that is determined by

$$\begin{aligned} F_s &= b \int_0^t \left(c + \frac{m_T}{b l_s} tan\phi\right)(1 - e^{-\frac{ix}{K}})\, dx \\ &= (A_s c + m_T tan\phi)\left[1 - \frac{K}{i l_s}(1 - e^{-\frac{i l_s}{K}})\right] \end{aligned}$$

which expresses the relationship among track slip, terrain values [16], vehicle geometry parameters and tractive effort. The previous analysis is applicable for predicting the tractive effort of tracked drive systems with uniform normal pressure distribution, which is rarely uniform in practical applications. Therefore, the developed area sensor can be used to evaluate the effect of normal multipeak pressure distribution.

D. Approaches for improved ICR location models

In contrast to the formalism for terrain description and motion modelling according the previous chapter, this paper attempts to predict vehicle motion by calculating the ICR of the track relative to the ground in order to measure instantaneous loads by usage of the introduced pressure sensor above. Conventional approaches are based on purely kinematic considerations as described in Fig. 6. The ICR

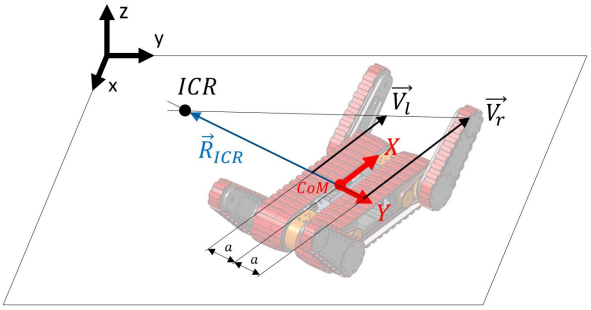

Fig. 6. Kinematics - Uniform Pressure Distribution

and the driving velocity vectors always lie in the XY plane of the body-fixed coordinate system (red), which is equal to the xy plane of the inertial coordinate system in Fig. 6. The position of the ICR results from the intersection of the CoM horizontal and the connecting straight line of the two velocity vectors $X = k \cdot Y + d$, i.e. the ICR is the zero point from the latter. Considering the velocities V_l and V_r as well as the distance a,

$$V_l = k \cdot (-a) + d \qquad V_r = k \cdot a + d \tag{5}$$

the corresponding linear equation in the body-fixed coordinate system is calculated as follows

$$k = -\frac{V_l - V_r}{2 \cdot a} \qquad d = \frac{V_l + V_r}{2} \tag{6}$$

$$X = -\frac{V_l - V_r}{2 \cdot a} \cdot Y + \frac{V_l + V_r}{2} \tag{7}$$

The zero of equation (7) coincides with the ICR. Hence,

$$X_{(R_{ICR,Y})} = 0 = -\frac{V_l - V_r}{2 \cdot a} \cdot R_{ICR,Y} + \frac{V_l + V_r}{2} \tag{8}$$

$$R_{ICR,Y} = a \cdot \frac{V_l + V_r}{V_l - V_r} \tag{9}$$

Finally the associated mathematical formulation of the ICR in relation to the body-fixed reference coordinate system is given by

$$\overrightarrow{R_{ICR}} = \begin{pmatrix} R_{ICR,X} \\ R_{ICR,Y} \end{pmatrix} = \begin{pmatrix} 0 \\ a \cdot \frac{V_l + V_r}{V_l - V_r} \end{pmatrix} \tag{10}$$

Weaknesses of this method become apparent in the case of uneven distribution of the contact load as well as increased slip between the belt and the environment. For example, when driving over an obstacle such as a wooden beam. In this case, the points of application of the velocity vectors can no longer be trivially assumed to be at the level of the CoM. This should be illustrated with Fig. 7. In this example, the

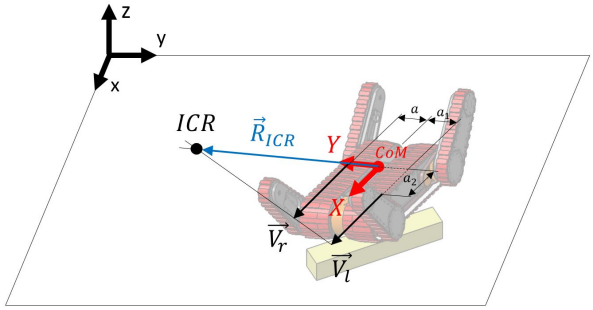

Fig. 7. Kinematics - Uneven Pressure Distribution

left velocity vector shifts forward due to the obstacle ahead. Thus, the linear equation is calculated by

$$V_l + a_2 = k \cdot (-a_1) + d \qquad V_r = k \cdot a + d \tag{11}$$

$$k = -\frac{V_l - V_r + a_2}{a + a_1} \qquad d = V_r + a \cdot \frac{V_l - V_r + a_2}{a + a_1} \tag{12}$$

$$X = -\frac{V_l - V_r + a_2}{a + a_1} \cdot Y + V_r + a \cdot \frac{V_l - V_r + a_2}{a + a_1} \tag{13}$$

Hence, the Y-distance of the ICR is obtained by

$$X_{(R_{ICR,Y})} = 0 = -\frac{V_l - V_r + a_2}{a + a_1} \cdot R_{ICR,Y} + V_r + a \cdot \frac{V_l - V_r + a_2}{a + a_1} \tag{14}$$

$$R_{ICR,Y} = a + \frac{V_r \cdot (a + a_1)}{V_l - V_r + a_2} \tag{15}$$

and the enhanced mathematical description of the ICR reads

$$\overrightarrow{R_{ICR}} = \begin{pmatrix} R_{ICR,X} \\ R_{ICR,Y} \end{pmatrix} = \begin{pmatrix} 0 \\ a + \frac{V_r \cdot (a + a_1)}{V_l - V_r + a_2} \end{pmatrix} \tag{16}$$

At this point it should be noted again that the ICR must always lie within the XY plane of the body-fixed coordinate system, but this no longer coincides with the xy plane of the inertial system. Extending the non-uniform load to the right track of the robot by using the parameters a_3 and a_4 instead of a, the procedure analogous to (11)-(16) leads to the final/general approach of calculating the ICR.

$$\overrightarrow{R_{ICR}} = \begin{pmatrix} R_{ICR,X} \\ R_{ICR,Y} \end{pmatrix} = \begin{pmatrix} 0 \\ a_3 + \frac{(V_r + a_4) \cdot (a_1 + a_3)}{V_l - V_r + a_2 - a_4} \end{pmatrix} \tag{17}$$

Conventional models do not offer the possibility to determine the unknown dimensions a_1, a_2, a_3 and a_4. Deviating from this, the integration of the measurement data of the pressure sensor enables the use of the improved model (17) for determining the points of contact of both tracks. This is achieved by calculating the center of gravity of the two tracks separately, using the measurement data of the pressure sensor and the local coordinates (x,y) of each of the 15x15 measurement points.

V. EXPERIMENTAL RESULTS

The sensor concept was tested and evaluated on different grounds and terrains. The experiments were based on the emerging standard test method apparatuses for response robots of the RoboCup Rescue League [17]. These test methods play an important role in the evaluation process of mobile UGVs and give participants, users and first responders a quick overview of how the individual robot systems perform in the areas of manoeuvring, mobility, dexterity and exploration [18],[19]. The proposed sensor concept provides the feedback about the pressure distribution and the localization of these pressure or support points. In addition to the distribution of the ground contact, the visualisations also show the centre of gravity of the respective area sensor (see black dot).

A. Flat Environment and Gravel

Most of the time indoor explorations are usually done on flat terrain or at hall transitions there are usually ledges or edge transitions.

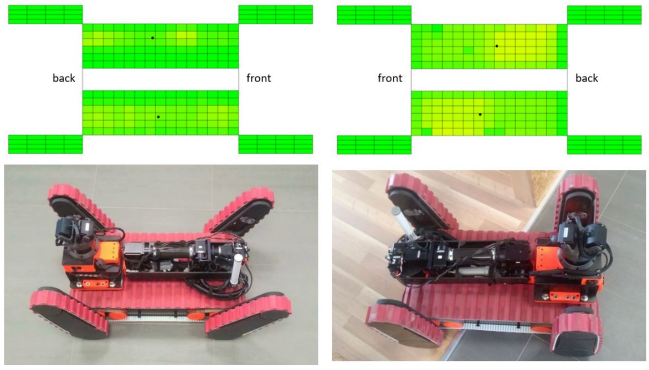

Fig. 8. Flat Environment

Fig. 8 perfectly illustrates the idea of the improved mathematical model for ICR determination using pressure sensor feedback. As already explained, the points of application of the velocity vectors corresponding to the environment are determined separately for each track. This is done by calculating the weighted centre of gravity per track. For this, one uses the individual measurement data as well as their corresponding local coordinates (x,y) of the 15x15 pressure sensor. The results of this calculation, i.e. the points of application of the velocity vectors, are shown throughout this chapter as black points per track. For approximately

uniformly distributed loads (Fig. 8 left), conventional approaches as described with Fig. 6 are sufficient, since the velocity vectors hardly deviate from the theoretical ideal consideration. For unevenly distributed pressure loads (Fig. 8/10 right), the use of the pressure sensor and the associated determination of the contact position offers an alternative way to predict the robot position (improved robot odometry) during rotations and advanced maneuvering.

In addition to solid surfaces, tests were also carried out on loose surfaces such as coarse gravel.

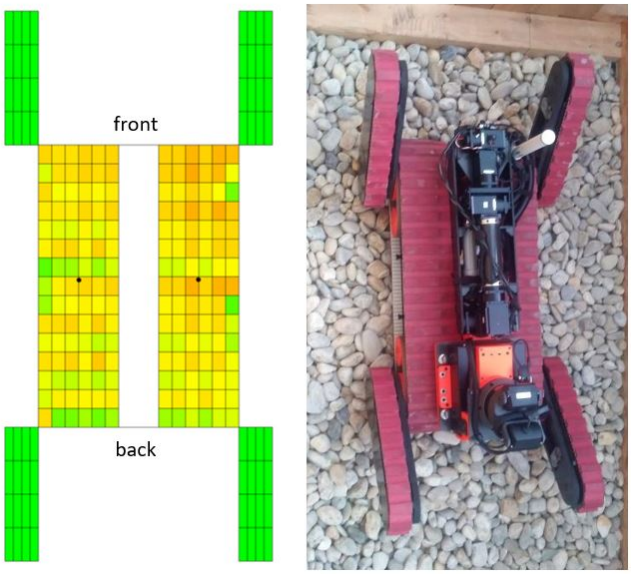

Fig. 9. Gravel

B. Bars

Bars are basic elements for testing the mobility of rescue robots on simple terrain. These objects can also be used as debris to test manipulation at the same time.

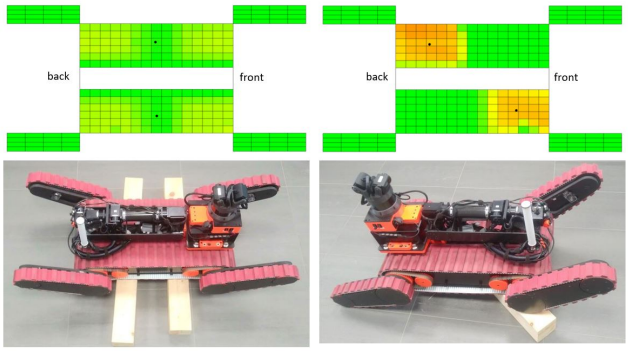

Fig. 10. Pressure distribution on bars

C. Hurdles and Stairs

Rescue robots will be tested to drive over terrain with medium to hard difficulty. Two 10 cm high rolling tube obstacles on top of each other for climbing up and down are actually no longer so easy to overcome for wheel-driven robots and already require a more all-terrain robot here. 45 degree stairs are also part of the test methods which are partly blocked with debris in the competitions.

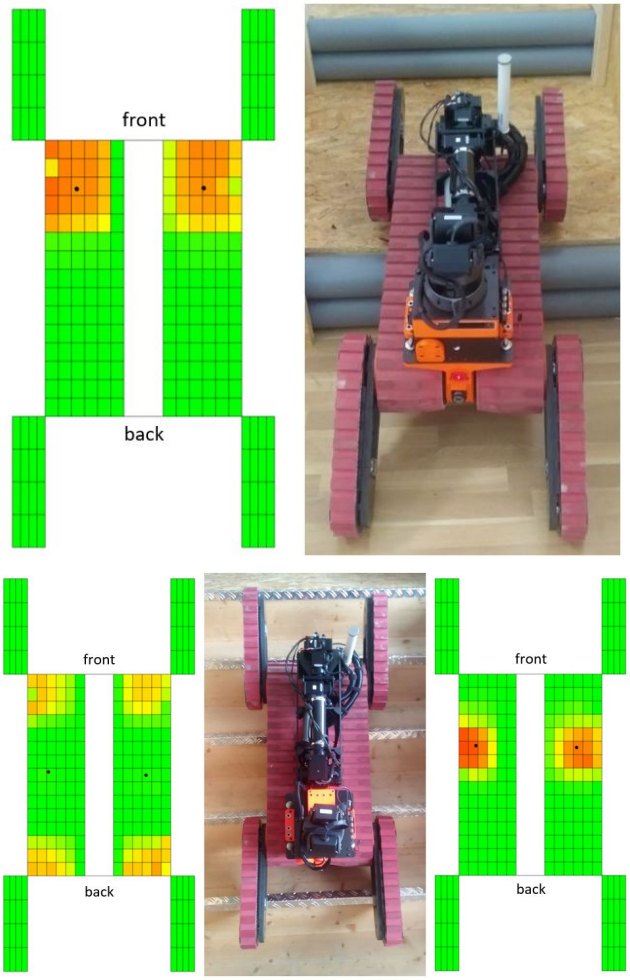

Fig. 11. Hurdles and Stairs

Fig. 11 above illustrates the contact points in the front area of the pressure sensor. These are shifted backwards accordingly during forward movement over hurdles. Fig. 11 below shows that different load situations are possible with stairs. On the left, it shows a moderate pressure distribution in the front and rear area of the pressure sensor. During the climb, however, local load peaks can also be expected due to one single step (right).

D. Different Terrain Conditions

During search and rescue applications, mobile robots are confronted with different terrain conditions. In order to simulate these with regard to sensor suitability, a further test course is being set up. To keep the track very common it includes obstacles and unevenness consisting of conventional bricks and wooden stairs, see Fig. 12 and Fig. 13. The appropriate sensor data are also shown graphically here, analogous to the preceding subsections of experimental results above.

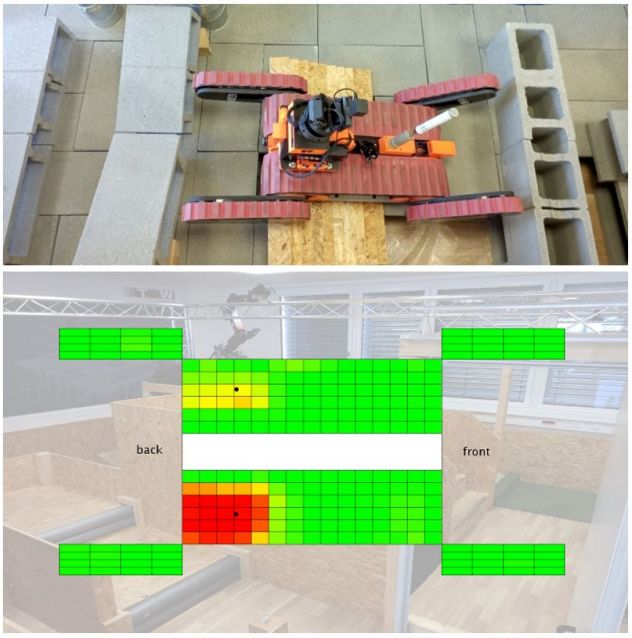

Fig. 12. Different Terrain Conditions (1)

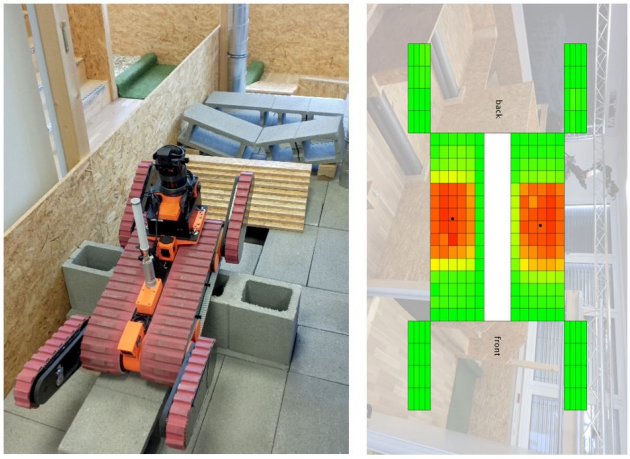

Fig. 13. Different Terrain Conditions (2)

VI. DISCUSSION AND FUTURE WORK

In this paper a tactile sensor system for tracked vehicles especially rescue robots is presented to improve the prediction of the resulting track forces and odometry calculation for tracked vehicles. In contrast to terrain descriptive formulations, the current contact force distribution is directly detected by this sensor system and can be used as a predictive model for tracked vehicle traversability in rough terrain. In addition to the feedback for the contact points an odometry calculation is applied to estimate the ICR locations of tracked vehicles in real time. Experimental results indicates that the proposed sensor system improves the traversability analysis and furthermore can be used for stability predictions of the system. In combination with online monitoring of the CoM during manipulation tasks in rough terrain safe operation and execution can be ensured.

A planned vehicle dynamic slip model for rough terrain which provides a more accurate prediction of longitudinal and lateral dynamics and a model for the distribution of vertical stresses for vehicle motion will be extended to include these attributes in future work.

REFERENCES

[1] M. Hutter, C. Gehring, A. Lauber, F. Gunther, C. D. Bellicoso, V. Tsounis, P. Fankhauser, R. Diethelm, S. Bachmann, M. Blösch, *et al.*, "Anymal-toward legged robots for harsh environments," *Advanced Robotics*, vol. 31, no. 17, pp. 918–931, 2017.

[2] X. A. Wu, T. M. Huh, R. Mukherjee, and M. Cutkosky, "Integrated ground reaction force sensing and terrain classification for small legged robots," *IEEE Robotics and Automation Letters*, vol. 1, no. 2, pp. 1125–1132, 2016.

[3] N. Seegmiller, F. Rogers-Marcovitz, G. Miller, and A. Kelly, "Vehicle model identification by integrated prediction error minimization," *The International Journal of Robotics Research*, vol. 32, no. 8, pp. 912–931, 2013.

[4] N. Seegmiller, F. Rogers-Marcovitz, G. Miller, and A. Kelly, "A unified perturbative dynamics approach to online vehicle model identification," in *Robotics Research*, pp. 585–601, Springer, 2017.

[5] J. Jiao, L. Sun, W. Kong, Y. Zhang, Y. Qiao, and C. Yuan, "A sliding parameter estimation method based on ukf for agricultural tracked robot," in *The 2014 2nd International Conference on Systems and Informatics (ICSAI 2014)*, pp. 277–282, IEEE, 2014.

[6] G. Yamauchi, K. Nagatani, T. Hashimoto, and K. Fujino, "Slip-compensated odometry for tracked vehicle on loose and weak slope," *Robomech Journal*, vol. 4, no. 1, pp. 1–11, 2017.

[7] J. Pentzer, S. Brennan, and K. Reichard, "Model-based prediction of skid-steer robot kinematics using online estimation of track instantaneous centers of rotation," *Journal of Field Robotics*, vol. 31, no. 3, pp. 455–476, 2014.

[8] G. Yamauchi, D. Suzuki, and K. Nagatani, "Online slip parameter estimation for tracked vehicle odometry on loose slope," in *2016 IEEE International Symposium on Safety, Security, and Rescue Robotics (SSRR)*, pp. 227–232, IEEE, 2016.

[9] H. Lu, G. Xiong, and K. Guo, "Motion predicting of autonomous tracked vehicles with online slip model identification," *Mathematical Problems in Engineering*, vol. 2016, 2016.

[10] J. Yi, J. Zhang, D. Song, and S. Jayasuriya, "Imu-based localization and slip estimation for skid-steered mobile robots," in *2007 IEEE/RSJ International Conference on Intelligent Robots and Systems*, pp. 2845–2850, IEEE, 2007.

[11] H. Zhao and Z. Wang, "Motion measurement using inertial sensors, ultrasonic sensors, and magnetometers with extended kalman filter for data fusion," *IEEE Sensors Journal*, vol. 12, no. 5, pp. 943–953, 2011.

[12] S.-T. Han, H. Peng, Q. Sun, S. Venkatesh, K.-S. Chung, S. C. Lau, Y. Zhou, and V. Roy, "An overview of the development of flexible sensors," *Advanced materials*, vol. 29, no. 33, p. 1700375, 2017.

[13] R. Edlinger and A. Nuechter, "Marc-modular autonomous adaptable robot concept," in *2019 IEEE International Symposium on Safety, Security, and Rescue Robotics (SSRR)*, pp. 1–7, IEEE, 2019.

[14] M. Bekker, "Introduction to terrain-vehicle systems," *University of Michigan Press*, vol. Ann Arbor, 1969.

[15] A. R. Reece, "Principles of soil-vehicle mechanics," *Proc. Institution of Mechanical Engineers*, vol. part 2A, 1965.

[16] J. Y. Wong, *Theory of ground vehicles*. John Wiley & Sons, 2008.

[17] R. Sheh, A. Jacoff, A.-M. Virts, T. Kimura, J. Pellenz, S. Schwertfeger, and J. Suthakorn, "Advancing the state of urban search and rescue robotics through the robocuprescue robot league competition," in *Field and service robotics*, pp. 127–142, Springer, 2014.

[18] T. Kimura, M. Okugawa, K. Oogane, Y. Ohtsubo, M. Shimizu, T. Takahashi, and S. Tadokoro, "Competition task development for response robot innovation in world robot summit," in *2017 IEEE International Symposium on Safety, Security and Rescue Robotics (SSRR)*, pp. 129–130, IEEE, 2017.

[19] A. Jacoff, R. Candell, A. Downs, H.-M. Huang, K. Kimble, K. Saidi, R. Sheh, and A. Virts, "Events for the application of measurement science to evaluate ground, aerial, and aquatic robots," in *2017 IEEE International Symposium on Safety, Security and Rescue Robotics (SSRR)*, pp. 131–132, IEEE, 2017.